Author version:*Estuar. Coast. Shelf Sci., vol.173; 2016; 79-92*

Residual estuarine circulation in the Mandovi, a monsoonal estuary: A three-dimensional model study

V. Vijith[a,1,*], S. R. Shetye[b], K. Baetens[c], P. Luyten[c], G. S. Michael[a]

[a] *CSIR - National Institute of Oceanography, Dona Paula, Goa 403004, India*
[b] *Goa University, Taleigao, Goa 403206, India*
[c] *Royal Belgian Institute of Natural Sciences (RBINS-MUMM), Gulledelle 100, 1200 Brussels, Belgium*

Abstract

Observations in the Mandovi estuary, located on the central west coast of India, have shown that the salinity field in this estuary is remarkably time-dependent and passes through all possible states of stratification (riverine, highly-stratified, partially-mixed and well-mixed) during a year as the runoff into the estuary varies from high values ($\sim 1000\ m^3 s^{-1}$) in the wet season to negligible values ($\sim 1\ m^3 s^{-1}$) at end of the dry season. The time-dependence is forced by the Indian Summer Monsoon (ISM) and hence the estuary is referred to as a monsoonal estuary. In this paper, we use a three-dimensional, open source, hydrodynamic, numerical model to reproduce the observed annual salinity field in the Mandovi. We then analyse the model results to define characteristics of residual estuarine circulation in the Mandovi. Our motivation to study this aspect of the Mandovi's dynamics is derived from the following three considerations. First, residual circulation is important to long-term evolution of an estuary; second, we need to understand how this circulation responds to strongly time-dependent runoff forcing experienced by a monsoonal estuary; and third, Mandovi is among the best studied estuaries that come under the influence of ISM, and has observations that can be used to validate the model. Our analysis shows that the residual estuarine circulation in the Mandovi shows four distinct phases during a year: a river like flow that is oriented downstream throughout the estuary; a salt-wedge type circulation, with flow into the estuary near the bottom and out of the estuary near the surface restricted close to the mouth of the estuary; circulation associated with a partially-mixed estuary; and, the circulation associated with a well-mixed

*Corresponding author
Email address: vijith@caos.iisc.ernet.in; vijithvnair@gmail.com (V. Vijith)
[1] Now at Centre for Atmospheric and Oceanic Sciences, Indian Institute of Science, Bangalore 560012, India

estuary. Dimensional analysis of the field of residual circulation helped us to establish the link between strength of residual circulation at a location and magnitude of river runoff and rate of mixing at the location. We then derive an analytical expression that approximates exchange velocity (bottom velocity minus near freshwater velocity at a location) as a function of freshwater velocity and rate of mixing.

Keywords: estuaries, residual circulation, salinity, numerical models, Mandovi, India

---

1. Introduction

The estuaries of India come under the influence of monsoon climate. The seasonal reversal of the atmospheric circulation over the North Indian Ocean and the Indian subcontinent is known as the monsoon. During the summer monsoon (June–September) winds blow from south-west and during the winter monsoon (November–May) from north-east. The summer monsoon winds are moisture laden and cause precipitation over the subcontinent. More than 70% of the annual rainfall over India ($\sim 0.9\ m$ on average) occur during the four months of the summer monsoon, often referred to as the Indian Summer Monsoon (ISM). There is very little rainfall over the country during the rest of the year, except for some parts of the east coast of India. There are spikes of high rainfall during active spells and lulls during breaks or weak spells of the ISM. Forced by the monsoon runoff, the Indian estuaries show marked differences in physical variables between the wet and the dry seasons. This is evident from seasonal variation in the vertical structure of salinity in the estuaries. The entire ecosystem and the associated natural habitat of an estuary also must adapt to this seasonality. Because of the seasonality, Indian estuaries are known as the *monsoonal estuaries*. The Mandovi (Figure 1) is a typical monsoonal estuary, located on the central west coast of India (Vijith et al., 2009; Vijith and Shetye, 2012).

Our objective in this paper is to examine an issue that is important to estuarine dynamics, but has not been addressed so far for any of the Indian monsoonal estuaries. The issue concerns estimation of sub-tidal along-channel circulation in the estuaries, usually called the residual estuarine circulation (Geyer and MacCready, 2014). It is broadly taken as the tidally averaged along-channel velocity field and has a net seaward transport at the surface and a net landward transport at the bottom. In practice tidal frequencies are filtered out to get the residual estuarine circulation. The nature of residual estuarine circulation determines the long-term

transport and distribution of salinity and materials such as sediments, phytoplanktons, larvae, pollutants etc. As noted by Stacey et al. (2001), while large fluxes are exchanged during a tidal cycle, it is the residual estuarine circulation that governs the net along-channel transport of salt and materials. This in turn determines the long-term evolution of an estuary.

Another consideration that makes determination of residual circulation in the Mandovi important is that, being a monsoonal estuary, it experiences large variation in forcing due to freshwater runoff during a year. It is important to determine how the residual circulation varies in response to the variation in forcing.

Yet another motivation is that we expect the pattern of residual circulation derived here for the Mandovi to be similar to that in many other Indian monsoonal estuaries, particularly those found along the west coast of India. These estuaries have geometries similar to that in the Mandovi and experience similar freshwater influx. The Mandovi is the best studied among them. Hence, it is the best suited for the study reported here because observations are available to validate the performance of the model that we have used here.

Burchard and Hetland (2010) give a brief history of earlier studies on determination of residual circulation in estuaries. In general, there are two major components that contribute to residual estuarine circulation: gravitational circulation arising from horizontal density gradient; and tidal straining. The pressure gradient due to along-channel density gradient, set up by the river runoff, drives a baroclinically-forced seaward directed surface flow and a landward directed bottom flow. This circulation, referred to as gravitational circulation, is assumed to be constant over a tidal cycle. Earlier estuarine classification schemes (Hansen and Rattray, 1965; Chatwin, 1976) were based on the assumption that gravitational circulation is the most important contributor to tidally averaged estuarine circulation. Hansen and Rattray (1965) defined two non-dimensional numbers, a circulation parameter and a stratification parameter, to investigate the strength of the gravitational circulation in estuaries. The circulation parameter was defined as the ratio of river induced velocity to root mean square tidal velocity. The stratification parameter was defined as the ratio of top to bottom salinity difference to mean salinity. Based on empirical data they concluded that the gravitation circulation is more vigorous when the values of these parameters are higher.

Jay and Smith (1990), using observations from the Columbia river estuary, argued that the predominant component of residual estuarine circulation is a steady gravitational circulation

and superimposed on it is spring-neap barotropic variations in mixing. A different mechanism, often referred to as tidal straining, was first proposed by Simpson et al. (1990) using an example from the Liverpool bay. They showed that during the flood tide, due to straining of horizontal density gradient, the water column destabilizes, increasing turbulent mixing and decreasing stratification and velocity shear. Whereas, during the ebb tide turbulent mixing decreases leading to an increase in stratification and velocity shear. During flood tide landward directed near-bottom currents increase due to mixing of momentum downwards, whereas, due to decreased mixing during ebb the seaward directed surface currents are intensified (Jay and Musiak, 1994). The velocity profile generated by tidal straining is similar to that of gravitational circulation. Burchard and Baumert (1998) using a numerical model and Stacey et al. (2001) using observations from the San Francisco bay showed that the component of tidal straining of residual estuarine circulation dominates the component of gravitational circulation. Later, Stacey et al. (2008), using a numerical water column model, showed that the tidal straining component of the residual circulation is strongly dependent on the timing of stratification within the tidal cycle.

Investigations on residual estuarine circulation have so far been conducted using observations (current meter, ADCP, etc.) and mathematical models (analytical or numerical). Examples of observational studies can be found in (Geyer et al., 2000) and (Ralston et al., 2008). Most of such empirical investigations have been guided by steady state analytical solutions of residual estuarine circulation. Some recent studies (see, for example, Brown et al. (2014)) have used observations in combination with three-dimensional numerical models. Vaz et al. (2009) is an example of the use of only a three-dimensional numerical model to infer residual estuarine circulation.

In this paper we use a three-dimensional numerical model of the Mandovi to infer the characteristics of residual estuarine circulation in the estuary, a strategy similar to the one adopted by Vaz et al. (2009). Here, we low-pass filter model simulated data to filter out tidal circulation to look into the annual evolution of residual estuarine circulation in the estuary.

The remainder of this paper is organized as follows. In the next section, we present a description of the Mandovi estuary and summarize the observational background of this research. Section 3 presents a description of the numerical model and its validation. The annual cycle of residual currents in the Mandovi estuary during three different periods of

runoff is examined in Section 4. These three periods are: 1) the wet period during the ISM; 2) the period of rapid decrease in runoff following withdrawal of ISM; and, 3) the period of very low runoff during the dry season. The relationship between residual circulation and runoff and vertical mixing for the Mandovi estuary is investigated in Section 5. Section 6 discusses limitations of our study and future work needed to take this research forward. Section 7 summarises the results.

2. The Mandovi estuary

The Mandovi estuary is located on the coastal plain of the central west coast of India, in the state of Goa (Figure 1a). The estuary is connected to another estuary, the Zuari, through the Cumbarjua canal. However, cross-sectional area of the canal is small enough to treat the two estuaries as independent systems. Shetye et al. (2007a) provide an overview of the Mandovi-Zuari estuarine system.

Based on the geometry, the Mandovi estuary can be divided into two parts. The first is a distinctively wide, 4 km long bay near the mouth where cross-sectional area decreases rapidly. The Second is an approximately 40 km long narrow-converging channel. The cross-sectional area here too decreases with distance from the mouth, but the rate of decrease is much smaller than that in the bay.

As seen in Figure 1a, a number of rivers join the Mandovi. The Mhadei River, the major supplier of runoff to the Mandovi estuary during the monsoon, and a smaller river Ragda join the Mandovi estuary near Ganjem (see Figure 1a), about 50 km from the mouth of the estuary. The Khandepar river, the biggest tributary of the Mandovi joins the Mandovi at Kulem. The average annual runoff at Ganjem and Kulem are $3400(\pm 648) \times 10^6\ m^3$ and $502(\pm 91) \times 10^6\ m^3$ respectively. A hydrological model study (Suprit, 2010) suggested, that runoff in the Mandovi doubles from head to mouth due to contributions from the tributaries. These contributions are: Khandepar (about 45% of the runoff measured at Ganjem); Valvat (about 25%; includes Dicholi and Kudnem rivers); and the Mhapsa (about 14%; includes Moide and Asnoda rivers). The rest of the 16% are contributed by other smaller rivulets. The total annual freshwater runoff into the Mandovi is about 40 times more than the volume of the estuary at the mean sea level ($145 \times 10^6\ m^3$).

Preferred position of Figure 1

Tides in the Mandovi are predominantly mixed semi-diurnal. They have been discussed in Sundar and Shetye (2005). Average tidal range during spring (neap) tide is 2.3 m (1.8 m).

Vijith et al. (2009) have described the annual cycle of salinity in the Mandovi estuary using observations carried out during 2007–08. These observations include fortnightly observation of a vertical section using a Conductivity Temperature Depth profiler (CTD) running along the length of the estuary from mouth to head covering a period of well over a year, and daily observation at one fixed location (near Panaji; see Figure 1) at a fixed time (1100 hours Indian Standard Time) during the day, also covering a similar period. The authors reported that because the estuary comes under the influence of ISM, the runoff in the estuary varies dramatically from very high values in the wet season to negligible values in the dry season. This gives the estuary its special characteristics: it exhibit stratification that varies between highly stratified salt-wedge type to partially-mixed to well-mixed estuary as the runoff goes through its annual cycle of variation. In essence the salinity field in the estuary is never in a steady state (Figure 2). The daily observations (Figure 3a–e) at Panaji showed that salinity falls sharply following a rain burst and rises during a lull in the monsoon. Slow but persistent increase in salinity occurred after withdrawal of the monsoon. Ingress of salinity into the estuary persisted throughout the dry season (approximately November–May). At the end of this season there is virtually no runoff into the estuary.

Vijith et al. (2009) also noted that the total runoff during the wet season is large, well over an order of magnitude larger than the estuarine volume, and that there are days when daily runoff in the Mandovi can exceed the volume of the estuary. It is expected that the Mandovi virtually turns into a river on such a day.

Superimposed on the annual pattern of salinity variation in the Mandovi described above is the neap spring asymmetry in salinity stratification, often seen in other estuaries too. Shetye et al. (2007b) have reported the difference in vertical stratification between a spring and a neap at one location in the channel of the Mandovi. The location was Old Goa (see the map in Figure 1). Time series of vertical structure of salinity in the middle of the channel at this location was recorded during the spring of 1 February 1999 and during the neap a week later on 8 February 1999. The observed fields at this time are shown in Figures 3g and i. These two days, being during the dry season, are times of low runoff. The tidal water level used in constructing the two figures was taken from the tide measured at the location. As seen in the

figure, the character of vertical stratification of the water column depended on the phase of the tide. The water column was well-mixed during flood and ebb phases of the tide due to high tidal velocities. The column was weakly stratified during slack water periods, when tidal currents weakened. The maximum stratification, i.e., the difference in salinity from surface to bottom, was about 1 during the spring. In contrast, the stratification was about 3 during the slack during the neap on 8 February 1999.

In putting together the 3D model described in the next section, we were motivated by the following considerations. First the basic framework of the model (numerics, for example) should have been well proven through implementation in other estuaries. Second, the model should be capable of reproducing the observations described in this section, in particular the annual cycle of salinity field. And, third, the model should allow us to analyse model output to infer on the relationship between residual circulation, freshwater influx and rate of vertical mixing. None of the 1D and 2D models of the Mandovi (see for example, Shetye and Murty (1987), Unnikrishnan and Manoj (2007) and Manoj and Unnikrishanan (2009)) have the ability to meet these three conditions. These models did not simulate the vertical structures of the salinity and other variables which are crucial for understanding the physical processes active in the estuary in general, and for studying the residual circulation in particular. We overcome this limitation by using a 3D model. Another motivation for the use of a 3D model arose from the complex geometry of the Mandovi-Zuari estuarine system. It is only with a 3D model that it is possible to infer the characteristics of alongshore fields that we discuss in Sections 4 and 5.

3. Numerical model

The numerical model used in this paper is based on COupled Hydrodynamic Ecological model for REgioNal Shelf seas (COHERENS), an open source, three dimensional, hydrodynamic, numerical model. COHERENS has been successfully employed in several estuaries and coastal seas: in the North sea (Baeye et al., 2012; Ponsar et al., 2011; Fettweis et al., 2010; Zintzen et al., 2008; Luyten et al., 2003), the Hervey Bay in Australia (Grawe et al., 2010), Port Kembla Harbour in Australia (Luick and Hinwood, 2008), the Spencer Gulf estuary in Australia (Kampf et al., 2010), the Scheldt estuary in the Netherlands (Arndt et al., 2011) and the Horsens Fjord in Denmark (Gustafsson and Bendtsen, 2007). The model has also

been used in many idealised theoretical studies (Kampf, 2012; Guillou and Chapalain, 2011; Kampf, 2009). See Luyten (2012) for detailed documentation and description of test cases of COHERENS.

Figure 1b shows the model domain and bathymetry. The model has a uniform grid resolution of 55 m with 751×521 grids and 5 vertical σ-levels. The model was run on a parallel SGI-Altix machine using 88 processors. A uniform bottom roughness length of 3.5×10^{-3} m was used to define the bottom stress. Total Variation Diminishing (TVD; Roe (1986)) scheme using the superbee limiter as a weighting function was used for advection. A second-order $k-\epsilon$ turbulence closure scheme was used for vertical diffusion. Horizontal diffusion was based on Smagorinsky scheme with Smagorinsky coefficient equal to 0.1. A drying and wetting scheme was applied. COHERENS employs a mode-splitting technique based on predictor-corrector method for time-stepping. 2D time-step permitted by CFL criteria was 1.6 s and a 3D time-step of 16 s was used. Output data were saved at hourly interval. The model was started from a state of rest with homogeneous initial salinity of 36. The start date was 1 June 2007, i.e., 6 days before onset of ISM that year.

Apart from the Boussinesq and hydrostatic assumptions used in COHERENS, we have also assumed a constant temperature (28° C) condition in the model throughout the simulation period and ignored meteorological forcings (wind stress and precipitation). In Section 1 of the supplementary material, we show that that these assumptions are reasonable.

A 10 km wide and 20 km long shelf sea was included to prescribe a steady salinity boundary condition of 36 at the western sea boundaries. This value of salinity was picked from data available in the region. Zero gradient of salinity was maintained at the northern and southern boundaries. Salinity at the river boundaries was always kept at zero. Though the model included both the Mandovi and Zuari estuaries, in this paper we focus on the Mandovi. Tidal boundary conditions at the coastal boundaries were extracted from global tidal solutions provided by Oregon State University Tidal Prediction Software (OTPS; http://volkov.oce.orst.edu/tides/otps.html). Ten tidal constituents were used: M_2, S_2, N_2, K_2, K_1, O_1, P_1, Q_1, Msf and Mm. Testut and Unnikrishnan (2014) note that global tidal solutions are inaccurate in some regions, $0-15$ km off the west coast of India. However, we have been able to simulate tides within the estuaries with good accuracy. RMS misfit for M_2 was about 4 cm (see Vijith (2014) for details). The runoff measured by the Central Water

Commission (CWC), India, at Ganjem was used to define the boundary condition at the head of the Mandovi (see Figure 3a). In addition to this, two other rivers, Khandepar and Valvat, with a total fresh water supply equivalent to 70% of the runoff at the head of the Mandovi was also included in the model. Following Suprit (2010) the runoffs due to the Valvat and Khandepar rivers were specified as 25% and 45% respectively of the value at the head of the Mandovi.

3.1. Validation of the simulated salinity field

A respectable numerical model of the Mandovi estuary, in addition to simulating the tides well, should simulate the major features of salinity variation that were discussed in Section 2. Among the important conditions that the model should fulfil are the following. First, the along-channel sections should reproduce the change in the salinity field that occurs with change in river runoff during the ISM. The sections should represent a river during intense spells of precipitation and highly-stratified condition near the mouth during lulls in the monsoon. The estuary should turn partially-mixed after withdrawal of the monsoon and well-mixed at the end of dry season in May. Second, the model should capture the rapid variations during the wet season (June–September) seen in the daily time series of salinity at Panaji. After withdrawal of the ISM, salinity at Panaji should increase slowly and exhibit the associated neap-spring oscillations. Average salinity of the water column should increase during spring tide and decrease during neap tide. Third, as seen in the observations (Section 2) the stratification in the channel should vary from a neap to a spring. Below we discuss how well the above three conditions are satisfied in the model.

Preferred position of Figure 2

In Figure 2 the observed along-channel sections in the Mandovi are compared with the sections as seen in the model. Note that observation of each along-channel section began at about 0800 hours in the morning and took about 4–5 hours to complete. Hence, we have used the model data at 1000 hours to compare with the observations in Figure 2. The figure shows that all the states of stratification observed in the Mandovi during different scenarios of river discharge are reproduced in the model. The almost complete flushing of the estuary on 10 August (b), the salt-wedges on 27 June and 24 August (a and c) and monotonic intrusion of salinity during the dry-season (e and f) as given by the model are virtually identical with

observed sections.

Figures 3b and 3c compare the modelled salinity at Panaji with the observed salinity at two depths at a station in Panaji. Observations were made at 1100 hours local time. Hence, the modelled salinities at 1100 hours are shown in Figure 3c. The overall pattern of time-series variation of salinity is well reproduced. Figure 3d compares the modelled and observed stratification at the station at Panaji, defined as the difference between the salinity at 5 m depth and salinity at the surface. Comparison of the time-series of the vertical profile of salinity at Panaji is shown in Figures 3e and 3f. The figures show that model captures the neap-spring difference in the average salinity of the water column at Panaji.

Preferred position of Figure 3

To examine if the model reproduces the neap-spring changes in stratification of the sort seen in the observations, described in Section 2 (Figures 3g and 3i), we picked a day-long model data from the location corresponding to the point where the observations shown in Figures 3g and 3i were made. The observations were made during 1 and 9 February 1999. The days picked up to compare are 21 and 28 February 2008 corresponding to spring and neap water-level variations that are similar to those seen in observations (Figures 3g and 3i). The model data are shown in Figures 3h and 3j. As seen in the figure, stratification i.e. the difference in salinity from surface to bottom, increased to as high as 3 during times of weak water-level variation during neap tide. The water column was well mixed during ebb and flood phases even during the neap tide (Figure 3j). The model results are, hence, consistent with observations.

More details about the model approximations, determination of the location of the open boundary and validation of tides and tidal currents are available in the supplementary material.

4. Residual estuarine circulation in the Mandovi

The along-channel model residual velocity was computed as follows. The x-components and y-components of velocities at every 0.5 km located along the middle of the main channel of the Mandovi was rotated to get the along-channel velocity. The angle of rotation was computed by minimizing the cross-channel velocity for a month (March) during dry season in a least square sense. The rotated along-channel velocities thus obtained were then low-pass

filtered with a third-order Butterworth filter with a cut-off period of 36 *hours* and then box-car smoothed with a 24 *hours* moving window. In order to remove the spatial noise a box-car smoother with a moving window of width 2.5 km was applied. We refer to the velocity field thus computed as the residual velocity field.

Because we expect stratification to increase (decrease) during neap (spring) when vertical mixing is weaker (stronger), whenever we discuss residual estuarine circulation in Sections 4.1 to 4.3 we also discuss vertical stratification seen in the salinity field. The salinity field was also filtered in the same way as the velocity field.

We examine along-channel residual velocity fields and the corresponding salinity fields during neaps and spring during three different periods: period with runoff greater than 100 m^3s^{-1} (next sub-section); with runoff between 10 m^3s^{-1} and 100 m^3s^{-1} (Sub-section 4.2); and, with runoff ~ 1 m^3s^{-1} (Sub-section 4.3).

Preferred position of Figures 4 and 5

4.1. The wet period with runoff >100 m^3s^{-1}

The along-channel residual velocity field on four occasions during the wet season is shown in Figure 4 (a–d). The intensity of the circulation depended on the intensity of the river runoff. On 30 June 2007, when the runoff was large (1706 m^3s^{-1}), the entire estuary experienced a seaward sub-tidal velocity greater than 1 ms^{-1} (Figure 4a). At the upstream end of the estuary the surface velocity was 1.5 ms^{-1} directed seaward. During this time the estuary was flushed with freshwater (Figure 5a) with condition within its channel similar to that in a river. On 22 July 2007 (Figure 5b), when the runoff was about (195 m^3s^{-1}), salinity intruded into the estuary at deeper levels as seen in Figures 4b and 5b. At this time the region near the mouth of the estuary was highly stratified. The seaward directed surface residual velocity was about 0.40 ms^{-1} and landward directed bottom residual velocity was about 0.10 ms^{-1}. The residual velocity field during the rest of the wet period was distinctly stronger during neaps (Figure 4d) than during the springs (Figure 4c). Simultaneously, the stratification was stronger during neaps (Figure 5d) than during the springs (Figure 5c).

Except for the conditions depicted in Figures 4a and 5a the residual estuarine circulation during this period consisted of salt-wedge type estuarine circulation. The salt-wedge as seen in the salinity field, was located near the mouth of the estuary. The circulation at this time, with

a distinct upstream flow near the bottom and a downstream flow in the surface, was restricted to a region of up to 10 km from the mouth of the estuary. The circulations strengthened (weakened) with approach of neaps (springs).

4.2. The period after withdrawal of the ISM with runoff in the range 10–100 m^3s^{-1}

During this period the magnitudes of the residual velocity decreased by an order of magnitude compared to the wet season. The surface and bottom residual velocities were about 5 $cm\ s^{-1}$. The circulation now became similar to what is associated with a partially-mixed estuary. As the season progressed, the residual estuarine circulation extended into the estuary. On 29 October 2007, the residual estuarine circulation was restricted to the region downstream of 15 km from the mouth (see Figure 4e); on 25 December 2007 it was seen upto 25 km from the mouth (see Figure 4g). The magnitude of residual estuarine circulation was higher during neaps than during springs. This can be seen by comparing Figures 4e and 4g with Figures 4f and 4h.

As runoff into the Mandovi estuary decreased, salinity intruded into the estuary. The 5 psu isohaline as seen in the lowpass filtered salinity section on 29 October 2007, when the runoff was 86 m^3s^{-1} (see Figure 5e), was located at 15 km from the mouth of the estuary. The isohaline intruded to about 21 km by 25 December 2007 when the runoff decreased to 57 m^3s^{-1} (see Figure 5g). The vertical structure of salinity showed that the estuary was more stratified during neap tides than during spring tides. For example, on 25 December 2007, when there was a spring tide, at a distance of 8 km from the mouth, bottom to surface salinity difference was 1.8 over a depth of 10 m; on 18 December 2007, during a neap tide, the difference was 4.0.

4.3. The period during dry season with runoff $\sim$ 1 m^3s^{-1}

During the dry season, runoff decreased to negligible levels in the Mandovi ($\sim$ 1 m^3s^{-1} on 1 March 2008). Salinity monotonically intruded into the estuary during the season. On 21 February 2008, when the runoff was 13 m^3s^{-1} the 5 psu isohaline was located at 29 km from the mouth of the estuary (see Figure 5i). On 16 April 2008 the 5 psu isohaline was seen at 34 km(see Figure 5l). Length of intrusion did not differ much between springs and neaps.

The magnitude of residual velocities decreased further from the previous period and were now in the range $1 - 5\ cms^{-1}$. On 21 February 2008, a well developed residual estuarine

circulation was seen upto about 35 km from the mouth of the estuary (see Figure 4i). On 16 April 2008, when the runoff decreased to 1 m^3s^{-1}, the residual estuarine circulation reached upto 40 km (see Figure 4l). Estuarine circulation was better developed during neaps than springs.

Overall, the circulation and stratification during this period were similar to the conditions that existed during the earlier period, except now the residual estuarine circulation was seen farther upstream, it was weaker, and the stratification too was weaker. The condition in the estuary was more like that in a well-mixed estuary than in a partially-mixed estuary of the period discussed in Section 4.2.

5. Residual estuarine circulation as a function of runoff and vertical mixing

We can summarise the salient characteristics of the simulated residual estuarine velocity field and the associated salinity field as follows:

1. The intensity of estuarine circulation, with residual velocity near the bottom oriented upstream and near-surface velocity oriented downstream, is controlled by magnitude of runoff and by amplitude of tidal variation. The latter influences vertical mixing in the estuary.
2. During periods of high ($\sim 100\ m^3s^{-1}$) runoff, the intensity of estuarine circulation is the largest and is similar to what has been associated with a salt-wedge. This circulation is restricted to about 10 km from the mouth. The high runoff turns the rest of the estuary into a river.
3. As runoff decreases, the intensity of estuarine circulation decreases and changes from salt-wedge type circulation (described in 2) to a partially-mixed type circulation to a well-mixed type circulation. Simultaneously, the extent of the residual estuarine circulation into the estuary increases.
4. Irrespective of magnitude of runoff, neaps have stronger estuarine circulation than springs.

The characteristics noted above are consistent with Figure 6 which shows the time-series of runoff, filtered rate of change of water level ($|\frac{dh}{dt}|$), filtered vertical turbulent diffusion coefficient of momentum (K_M), which is used here as a measure for intensity of vertical mixing, and residual velocities at the bottom and at the surface. In the model, K_M was obtained from

a turbulence model obtained from Reynolds Averaged Navier-Stokes (RANS) equations. The parameterization of vertical diffusion coefficients contains the turbulent energy (k) and its dissipation (ϵ) as variables (see Luyten (2012) for details).

Preferred position of Figure 6

In Figure 6, at each location a minimum in K_M coincides with a maximum in magnitude of both surface and bottom velocities. That is, when vertical mixing decreases, residual estuarine circulation increases. This holds at all times except for extreme runoff, in which case strong downstream velocities occur that are directly related to the runoff. In Figure 6 it can be also seen that during the dry season the pattern of K_M is similar to that of $|\frac{dh}{dt}|$, where h is the height of water surface and t is time. Earlier studies have shown that vertical mixing is proportional to magnitude of tidal velocity or amplitude of tidal elevation (Bowden, 1967; Ianniello, 1977).

In essence, Figure 6 implies that the residual estuarine circulation at a location in the Mandovi is dependent on runoff and vertical mixing at that location. That is, we expect that the first of the following three variables can be expressed as a function of the remaining two:

1. Magnitude of residual estuarine circulation at a location: we use near-bottom velocity (u_b) as a measure of this variable.
2. Magnitude of vertical mixing at the same location: we use filtered K_M as a measure of this variable. The filtering of K_M was done in the same way as that of the residual velocity, i.e. a third-order low-pass Butterworth filter with a cut-off period of 36 *hours* was used.
3. Magnitude of runoff at the location: we use the velocity induced by runoff at the location (u_R), runoff divided by area of cross-section of the channel at the location, to represent the variable.

We further expect that the following five variables will play a role in the above relationship: g, H, β, s_0 and u_T^*. Here g is the acceleration due to gravity, H is the mean depth of the estuary, β is the salinity expansion coefficient, u_T^* is the maximum tidal velocity in the estuary, and s_0 is the average ocean salinity. We thus have eight physical variables (u_b, u_R, K_M, g, H, β, s_0 and u_T^*) in two dimensions (length and time). We can therefore construct 6 non-dimensional variables: u_b/u_T^*, $K_M/(u_T^* H)$, $u_R/(\beta s_0 g H)^{1/2}$, $u_T^*/(\beta s_0 g H)^{1/2}$, β and s_0. The

Buckingham's Π theorem then implies that

$$u_b/u_T^* = f(K_M/(u_T^* H), u_R/(\beta s_0 g H)^{1/2}, u_T^*/(\beta s_0 g H)^{1/2}, \beta, s_0) \quad (1)$$

Of the five variables on the right hand side of Equation 1, three ($u_T^*/(\beta s_0 g H)^{1/2}$, β and s_0) are constants. Hence, we have

$$u_b/u_T^* = f(K_M/(u_T^* H), u_R/(\beta s_0 g H)^{1/2}) \quad (2)$$

The second number on the right hand side of Equation 2 is often referred to as freshwater Froude number (F_R; Geyer and MacCready (2014)). It is the ratio of river-induced velocity to maximum possible frontal propagation speed. We refer to the first number as the mixing number (M). It is the ratio of vertical eddy diffusivity to a scale of mixing due to horizontal component of tidal velocity ($u_T^* H$). We therefore rewrite Equation 2 as

$$u_b \sim f(M, F_R) \quad (3)$$

where, $M = K_M/(u_T^* H)$ and $F_R = u_R/(\beta s_0 g H)^{1/2}$.

We take, $g = 9.8\ ms^{-2}$, $H = 5\ m$, $\beta = 7.7 \times 10^{-4}$, $s_0 = 36$ and $u_T^* = 1\ ms^{-1}$. u_R is obtained by dividing river runoff (R) with area of cross-section (A) at each location.

Preferred position of Figure 7

The relationship depicted in Equation 3 should hold at any location in the estuary. In Figure 7 we have plotted u_b as a function of mixing number (M) and freshwater Froude number (F_R) using model data at a dozen locations in the Mandovi estuary. The distances of these locations from the mouth are between 2.5 km and 35 km. Each figure in Figure 7 (and in Figure 8) is drawn using low-pass filtered values of M, F_R and u_b ($u_b - u_R$ in Figure 8b) at each location at every hour for a year. Thus, at any location we could get 8760 data points. Of these 740 points during the first month of simulation were discarded to eliminate the impact of initial conditions. Another thousand points which were located away from main region of interest, i.e., $0 < M < 1.75 \times 10^{-3}$ and $0 < F_R < 0.2$, were also discarded. Hence, each of the figures in Figures 7 and 8 have about 7000 data points (more information on data points used to construct Figures 7b and 8 is given in the supplementary material).

In each of the dozen figures in Figure 7 as F_R increases, the bottom velocity u_b also increases. Note that u_b is positive when directed in the upstream direction. It turns negative when the runoff overwhelms the estuarine circulation.

Of all the 12 figures in Figure 7, Figure 7b, which represents the conditions at 5.5 km from the mouth of the Mandovi estuary, is the most informative. At this location the estuary experiences all the four phases: riverine when runoff is very high; salt-wedge-like when the runoff is high; partially-mixed; and well-mixed (see Figures 4 and 5). As a result, Figure 7b permits us to delineate regions in (M, F_R) space that mark transition through these phases at the location. The region $u_b < 0$ marks the riverine phase of the estuary at the location. The line that marks the points in (M, F_R) plane with maximum u_b (as function of F_R) is shown in Figure 7b with a dashed line. For a given rate of mixing, i.e., for a given value of M, as runoff increases (i.e., F_R increases) from the condition $F_R = 0$, u_b increases (the estuarine circulation strengthens) till it reaches the maximum (the dashed line). As F_R increases further the riverine unidirectional flow begins to dominate over the estuarine circulation. As a result u_b decreases. This behaviour continues till F_R is high enough to make u_b vanish. As F_R increases further the flow becomes downstream everywhere and the estuarine circulation is overwhelmed by river flow.

Figure 7b (and some of the other frames in Figure 7) has three distinct domains. The first domain is bounded by F_R equal to 0 and by the dashed line in the figure. The domain covers almost the entire range of M. The second domain is bounded by the dashed line and the contour of zero bottom velocity (u_b). Again the domain covers most of the range of M. The third domain is covered by the blue area where the velocity is negative, i.e. out of the estuary at the bottom of the channel. In the first domain, residual estuarine circulation intensifies as the runoff into the estuary increases for a given rate of vertical mixing. The second domain represents the state where the residual estuarine circulation gets pushed out due to increase in runoff. The third domain represents the condition when the estuary turns into a river due to very high runoff. In this domain the velocity everywhere is oriented towards the mouth of the estuary.

Figures 7g–l represent conditions that occur at locations farther upstream from near the mouth. At these locations the residual estuarine circulation is of type found in partially- or well-mixed estuaries, and it exists only when runoff is below a certain threshold. Above the threshold the circulation turns riverine. That means the domains found in Figures 7g–l are of the second or third type of the three domains of Figures 7a–f discussed earlier.

Preferred position of Figure 8

An expanded version of Figure 7b, with the three domains described above, is shown in Figure 8a. This figure allows us to examine estuarine circulation as a function of (M, F_R) from another perspective arising from the following consideration. The use of u_b as a measure for the residual estuarine circulation can be questioned on the ground that this velocity also contains the near-bottom velocity induced by runoff (u_R). It has been suggested that a better measure of residual estuarine circulation is $u_E = u_b - u_R$. This term, often referred to as exchange flow, is another measure of residual estuarine circulation, and of two-layer estuarine flow (Geyer and MacCready, 2014). Figure 8b shows u_E at the same location as in Figure 8a, i.e. at 5.5 km upstream of the mouth. Although, the boundaries separating the three domains are not clear in this figure, it shows that u_E decreases as mixing increases for all values of F_R. The nature of the contours of u_E in the figure suggests that a simple mathematical fit is possible. i.e., u_E can be expressed as a function of M and F_R. By trial and error we found that the following simple expression is a good approximation to the relationship between u_E, F_R and M seen in Figure 8b.

$$u_E = (a_1 + a_2 F_R)/(a_3 + a_4 M) \tag{4}$$

Here $a_i, i = 1, 2, 3, 4$ are four constant coefficients. For the best fit shown in Figure 8c, the coefficient values are, respectively, $44, 1.2 \times 10^3,\ 5.5 \times 10^2$ and 1.1×10^6. It may be noted that the above coefficients are satisfied only at this particular location in the estuary and a different location could have a different set of coefficients.

Equation 4 is consistent with the scaling equation given by MacCready and Geyer (2010) in which, $u_E = (g\beta H^3 \partial\overline{s}/\partial x)/48K_M$. In Equation 4 the salinity gradient is represented by a linear function of freshwater runoff. Both, Equation 4 and the equation given MacCready and Geyer (2010) imply that u_E decreases with increase in mixing. An early empirical evidence for this, from Admiralty inlet Puget Sound, has been reported in Geyer and Cannon (1982). Whenever K_M is higher, we expect more intense vertical mixing, which in turn should decrease residual estuarine circulation. A lower value of K_M represents lower vertical mixing and stronger residual estuarine circulation.

6. Discussion

As noted in the Introduction, this is the first time the residual estuarine circulation in Indian monsoonal estuaries is being examined. The study has led to important inferences, such as Equation 4. It is important that we examine the limitations of these results and comment on future work to take this research forward.

The most important forcing function of monsoonal estuary is freshwater runoff. Most of the Indian rivers are poorly gauged. The Mandovi has only one gauge, at Ganjem, that provided the daily mean values that were used to define the freshwater influx at the upstream end of the main channel of the Mandovi. At the upstream ends of the other rivers that provide freshwater to the estuary we have used scaled down values derived from the Ganjem gauge. We feel that this is a reasonable approximation because the hydrological model of the catchment area of the Mandovi-Zuari estuaries (Suprit, 2010) is consistent with the approximation. Nevertheless, it is an approximation and getting runoff data recorded with gauges is highly desirable. Such data will help determine the limitations on the freshwater forcing used in the model.

Future work must also examine how well the relationship between residual estuarine circulation, freshwater runoff and mixing, that was discussed in the previous section holds in the field data. At present, there are no current meter observations available in the Mandovi and Zuari estuaries to estimate residual estuarine circulation. Collecting them would be the next logical step towards formulation of a theoretical framework for understanding Indian monsoonal estuaries.

Future work will also need to examine implications of this study to the estuarine ecosystem. An important estuarine variable with implications to the ecosystem is the estuarine residence time. How does it change as the estuary switches from one mode of residual circulation to another?

In essence, this study marks a step that will need to be followed by others to evolve a holistic understanding of Indian monsoonal estuaries

7. Summary

In this paper we have used an open-source, hydrodynamic, numerical system (COHERENS) to model the Mandovi estuary. To our knowledge, it is for the first time it has been shown

that the annual cycle of salinity as recorded in the observation is well reproduced in a model of an Indian monsoonal estuary. The model uses a three-dimensional, fine resolution grid ($55\ m \times 55\ m$) and includes a part of the shelf sea. The model is capable of simulating various vertical structures of the salinity field that occurs in a monsoonal estuary during a year, especially during the wet season, when advective processes are dominant.

Preferred position of Figure 9

In Vijith et al. (2009) and Vijith and Shetye (2012), using the observed salinity field, we argued that monsoonal estuaries exhibit conditions that vary from season to season depending on the runoff into the estuary. It was found that the Mandovi estuary can have conditions that vary from highly-stratified to partially-mixed to well-mixed. In the present paper we have arrived at a similar inference based on the variability seen in residual estuarine circulation. We have shown that the residual estuarine circulation inferred from our numerical model implies that the residual estuarine circulation in the Mandovi varies from riverine to salt-wedge to partially-mixed type to well-mixed type. Figure 9 provides a schematic that summarises the varying state of residual estuarine circulation experienced during its annual cycle. This schematic together with the relationship between residual circulation, runoff and mixing as shown in Figure 8 and depicted in Equation 4 summarise the special features of dynamics of monsoonal estuaries.

Acknowledgements

We thank D.G. Bowers, Eric Wolanski and two anonymous reviewers for their comments that helped in improving the manuscript significantly. V.V. acknowledges travel grant from the Council of Scientific and Industrial Research (CSIR), India. V.V., K.B. and P.L. acknowledge support from CEBioS programme of the Royal Belgian Institute of Natural Sciences (RBINS), Belgium. The High Performance Computing (HPC) facility used for carrying out the simulation is located at CSIR-4PI (formerly CSIR-CMMACS), Bangalore. Test runs were performed in an HPC located at INCOIS, Hyderabad. Help from R.P Thangavelu (CSIR-4PI), Ashapurna Marndi (CSIR-4PI), S.S.C. Shenoi (INCOIS) and K. Annapoornaiah (INCOIS) is acknowledged. We thank K. Haris at CSIR-NIO for his help in the preparation of Figure 9. Generic Mapping Tools (GMT), Ferret, FORTRAN, Python, LaTeX and Google were exten-

sively used. This work was a part of V.V.'s doctoral research carried out at CSIR-NIO, Goa. This is NIO contribution XXXX.

References

Arndt, S., Lacroix, G., Gypens, N., Regnier, P., Lancelot, C., 2011. Nutrient dynamics and phytoplankton development along an estuary-coastal zone continuum: A model study. Journal of Marine Systems 84, 49 – 66. doi:http://dx.doi.org/10.1016/j.jmarsys.2010.08.005.

Baeye, M., Fettweis, M., Legrand, S., Dupont, Y., Lancker, V.V., 2012. Mine burial in the seabed of high-turbidity area-findings of a first experiment. Continental Shelf Research 43, 107 – 119. doi:http://dx.doi.org/10.1016/j.csr.2012.05.009.

Bowden, K.F., 1967. Stability effects on turbulent mixing in tidal currents. Physics of Fluids (1958-1988) 10, S278–S280. doi:http://dx.doi.org/10.1063/1.1762468.

Brown, J., Bolanos, R., Souza, A., 2014. Process contribution to the time-varying residual circulation in tidally dominated estuarine environments. Estuaries and Coasts 37, 1041–1057. doi:http://dx.doi.org/10.1007/s12237-013-9745-6.

Burchard, H., Baumert, H., 1998. The formation of estuarine turbidity maxima due to density effects in the salt wedge. a hydrodynamic process study. Journal of Physical Oceanography 28, 309–321. doi:http://dx.doi.org/10.1175/1520-0485(1998)028<0309:TFOETM>2.0.CO;2.

Burchard, H., Hetland, R.D., 2010. Quantifying the contributions of tidal straining and gravitational circulation to residual circulation in periodically stratified tidal estuaries. Journal of Physical Oceanography 40, 1243–1262. doi:http://dx.doi.org/10.1175/2010JPO4270.1.

Chatwin, P., 1976. Some remarks on the maintenance of the salinity distribution in estuaries. Estuarine and Coastal Marine Science 4, 555 – 566. doi:http://dx.doi.org/10.1016/0302-3524(76)90030-X.

Fettweis, M., Francken, F., den Eynde, D.V., Verwaest, T., Janssens, J., Lancker, V.V., 2010. Storm influence on SPM concentrations in a coastal turbidity maximum area with high

anthropogenic impact (southern North Sea). Continental Shelf Research 30, 1417 – 1427. doi:http://dx.doi.org/10.1016/j.csr.2010.05.001.

Geyer, W.R., Cannon, G.A., 1982. Sill processes related to deep water renewal in a fjord. Journal of Geophysical Research: Oceans 87, 7985–7996. doi:http://dx.doi.org/10.1029/JC087iC10p07985.

Geyer, W.R., MacCready, P., 2014. The estuarine circulation. Annual Review of Fluid Mechanics 46, 175–197. doi:http://dx.doi.org/10.1146/annurev-fluid-010313-141302.

Geyer, W.R., Trowbridge, J.H., Bowen, M.M., 2000. The dynamics of a partially mixed estuary. Journal of Physical Oceanography 30, 2035–2048. doi:http://dx.doi.org/10.1175/1520-0485(2000)030<2035:TDOAPM>2.0.CO;2.

Grawe, U., Wolff, J.O., Ribbe, J., 2010. Impact of climate variability on an east Australian bay. Estuarine, Coastal and Shelf Science 86, 247 – 257. doi:http://dx.doi.org/10.1016/j.ecss.2009.11.020.

Guillou, N., Chapalain, G., 2011. Effects of waves on the initiation of headland-associated sandbanks. Continental Shelf Research 31, 1202 – 1213. doi:http://dx.doi.org/10.1016/j.csr.2011.04.013.

Gustafsson, K.E., Bendtsen, J., 2007. Elucidating the dynamics and mixing agents of a shallow fjord through age tracer modelling. Estuarine, Coastal and Shelf Science 74, 641 – 654. doi:http://dx.doi.org/10.1016/j.ecss.2007.05.023.

Hansen, D.V., Rattray, M., 1965. Gravitational circulation in straits and estuaries. Journal of Marine Research 23, 104–122.

Ianniello, J., 1977. Non-linearly induced residual currents in tidally dominated estuaries. Ph.D. Thesis. The University of Connecticut.

Jay, D.A., Musiak, J.D., 1994. Particle trapping in estuarine tidal flows. Journal of Geophysical Research: Oceans 99, 20445–20461. doi:http://dx.doi.org/10.1029/94JC00971.

Jay, D.A., Smith, J.D., 1990. Residual circulation in shallow estuaries: 2. weakly stratified and partially mixed, narrow estuaries. Journal of Geophysical Research: Oceans 95, 733–748. doi:http://dx.doi.org/10.1029/JC095iC01p00733.

Kampf, J., 2009. On the interaction of time-variable flows with a shelfbreak canyon. Journal of Physical Oceanography 39, 248–260. doi:http://dx.doi.org/10.1175/2008JPO3753.1.

Kampf, J., 2012. Lee effects of localized upwelling in a shelf-break canyon. Continental Shelf Research 42, 78 – 88. doi:http://dx.doi.org/10.1016/j.csr.2012.05.005.

Kampf, J., Payne, N., Malthouse, P., 2010. Marine connectivity in a large inverse estuary. Journal of Coastal Research 26, 1047–1056. doi:http://dx.doi.org/10.2112/JCOASTRES-D-10-00043.1.

Luick, J.L., Hinwood, J.B., 2008. Water levels in a dual-basin harbour in response to infragravity and edge waves. Progress in Oceanography 77, 367 – 375. doi:http://dx.doi.org/10.1016/j.pocean.2006.04.002.

Luyten, P., 2012. A coupled hydrodynamical-ecological model for regional and shelf seas: User documentation, Version 2.1.2. On-line documentation 1193 pp. Royal Belgian Institute for Natural Sciences - Management Unit of the North sea Mathematical Models (RBINS-MUMM). MUMM, Gulledelle 100, B-1200 Brussels, Belgium. URL: `http://www2.mumm.ac.be/coherens/documentation.php`.

Luyten, P.J., Jones, J.E., Proctor, R., 2003. A numerical study of the long- and short-term temperature variability and thermal circulation in the North sea. Journal of Physical Oceanography 33, 37 – 56. doi:http://dx.doi.org/10.1175/1520-0485(2003)033<0037:ANSOTL>2.0.CO;2.

MacCready, P., Geyer, W.R., 2010. Advances in estuarine physics. Annual Review of Marine Science 2, 35–58. doi:http://dx.doi.org/10.1146/annurev-marine-120308-081015.

Manoj, N.T., Unnikrishanan, A.S., 2009. Tidal circulation and salinity distribution in the Mandovi and Zuari estuaries: Case study. Journal of Waterway, Port, Coastal, and Ocean Engineering 135, 278–287. doi:http://dx.doi.org/10.1061/(ASCE)0733-950X(2009)135:6(278).

Ponsar, S., Luyten, P., Ozer, J., 2011. Combined model state and parameter estimation with an ensemble Kalman filter in a North Sea station 1-D numerical model. Ocean Dynamics 61, 1869–1886. doi:http://dx.doi.org/10.1007/s10236-011-0477-5.

Ralston, D.K., Geyer, W.R., Lerczak, J.A., 2008. Subtidal salinity and velocity in Hudson River estuary: Observations and modeling. Journal of Physical Oceanography 38, 753–770. doi:http://dx.doi.org/10.1175/2007JPO3808.1.

Roe, P.L., 1986. Characteristic-based schemes for the euler equations. Annual Review of Fluid Mechanics 18, 337–365. doi:http://dx.doi.org/10.1146/annurev.fl.18.010186.002005.

Shetye, S.R., Dileep Kumar, M., Shankar, D. (Eds.), 2007a. The Mandovi and Zuari estuaries. National Institute of Oceanography, Goa.

Shetye, S.R., Michael, G.S., Viswas, C.P., 2007b. Mixing and intrusion of salt, in: Shetye, S.R., Dileep Kumar, M., Shankar, D. (Eds.), The Mandovi and Zuari estuaries. National Institute of Oceanography, Goa. chapter 4.

Shetye, S.R., Murty, C.S., 1987. Seasonal variation of salinity in the Zuari estuary, Goa, India. Proceedings of the Indian Academy of Sciences (Earth and Planetary Sciences) 96, 249–257. doi:http://dx.doi.org/10.1007/BF02841617.

Shetye, S.R., Shankar, D., Neetu, S., Suprit, K., Michael, G.S., Chandramohan, P., 2007c. The environment that conditions the Mandovi and Zuari estuaries, in: Shetye, S.R., Dileep Kumar, M., Shankar, D. (Eds.), The Mandovi and Zuari estuaries. National Institute of Oceanography, Goa. chapter 1.

Simpson, J., Brown, J., Matthews, J., Allen, G., 1990. Tidal straining, density currents, and stirring in the control of estuarine stratification. Estuaries 13, 125–132. doi:http://dx.doi.org/10.2307/1351581.

Sindhu, B., Suresh, I., Unnikrishnan, A.S., Bhatkar, N.V., Neetu, S., Michael, G.S., 2007. Improved bathymetric datasets for the shallow water regions in the Indian ocean. Journal of Earth System Science 116, 261–274. doi:http://dx.doi.org/10.1007/s12040-007-0025-3.

Stacey, M.T., Burau, J., Monismith, S.G., 2001. Creation of residual flows in a partially stratified estuary. Journal of Geophysical Research 106, 17013–17037. doi:http://dx.doi.org/10.1029/2000JC000576.

Stacey, M.T., Fram, J.P., Chow, F.K., 2008. Role of tidally periodic density stratification in the creation of estuarine subtidal circulation. Journal of Geophysical Research: Oceans 113. doi:http://dx.doi.org/10.1029/2007JC004581. c08016.

Sundar, D., Shetye, S.R., 2005. Tides in the Mandovi and Zuari estuaries, Goa, west coast of India. Journal of Earth System Science 114, 493–503. doi:http://dx.doi.org/10.1007/BF02702025.

Suprit, K., 2010. Hydrological modelling of the west coast of India. Ph.D. Thesis. Goa University. Goa University, Talegao, Goa.

Testut, L., Unnikrishnan, A.S., 2014. Improving modeling of tides on the continental shelf off the west coast of India. Journal of Coastal Research (accepted for publication) doi:http://dx.doi.org/10.2112/JCOASTRES-D-14-00019.1.

Unnikrishnan, A.S., Manoj, N.T., 2007. Numerical models, in: Shetye, S.R., Kumar, M.D., Shankar, D. (Eds.), The Mandovi and Zuari estuaries. National Institute of Oceanography, Goa. chapter 03.

Vaz, N., Dias, J.M., Leitao, P.C., 2009. Three-dimensional modelling of a tidal channel: The espinheiro channel (portugal). Continental Shelf Research 29, 29 – 41. doi:http://dx.doi.org/10.1016/j.csr.2007.12.005.

Vijith, V., 2014. Physical oceanography of the Mandovi and Zuari, two monsoonal estuaries in Goa, central west coast of India. Ph.D. Thesis. Goa University. Goa University, Talegao, Goa.

Vijith, V., Shetye, S.R., 2012. A stratification prediction diagram from characteristics of geometry, tides and runoff for estuaries with a prominent channel. Estuarine, Coastal and Shelf Science 98, 101–107. doi:http://dx.doi.org/10.1016/j.ecss.2011.12.006.

Vijith, V., Sundar, D., Shetye, S.R., 2009. Time-dependence of salinity in monsoonal estuaries. Estuarine, Coastal and Shelf Science 85, 601–608. doi:http://dx.doi.org/10.1016/j.ecss.2009.10.003.

Zintzen, V., Norro, A., Massin, C., Mallefet, J., 2008. Spatial variability of epifaunal communities from artificial habitat: Shipwrecks in the Southern Bight of the North Sea. Estuarine, Coastal and Shelf Science 76, 327 – 344. doi:http://dx.doi.org/10.1016/j.ecss.2007.07.012.

List of Figures

Figures

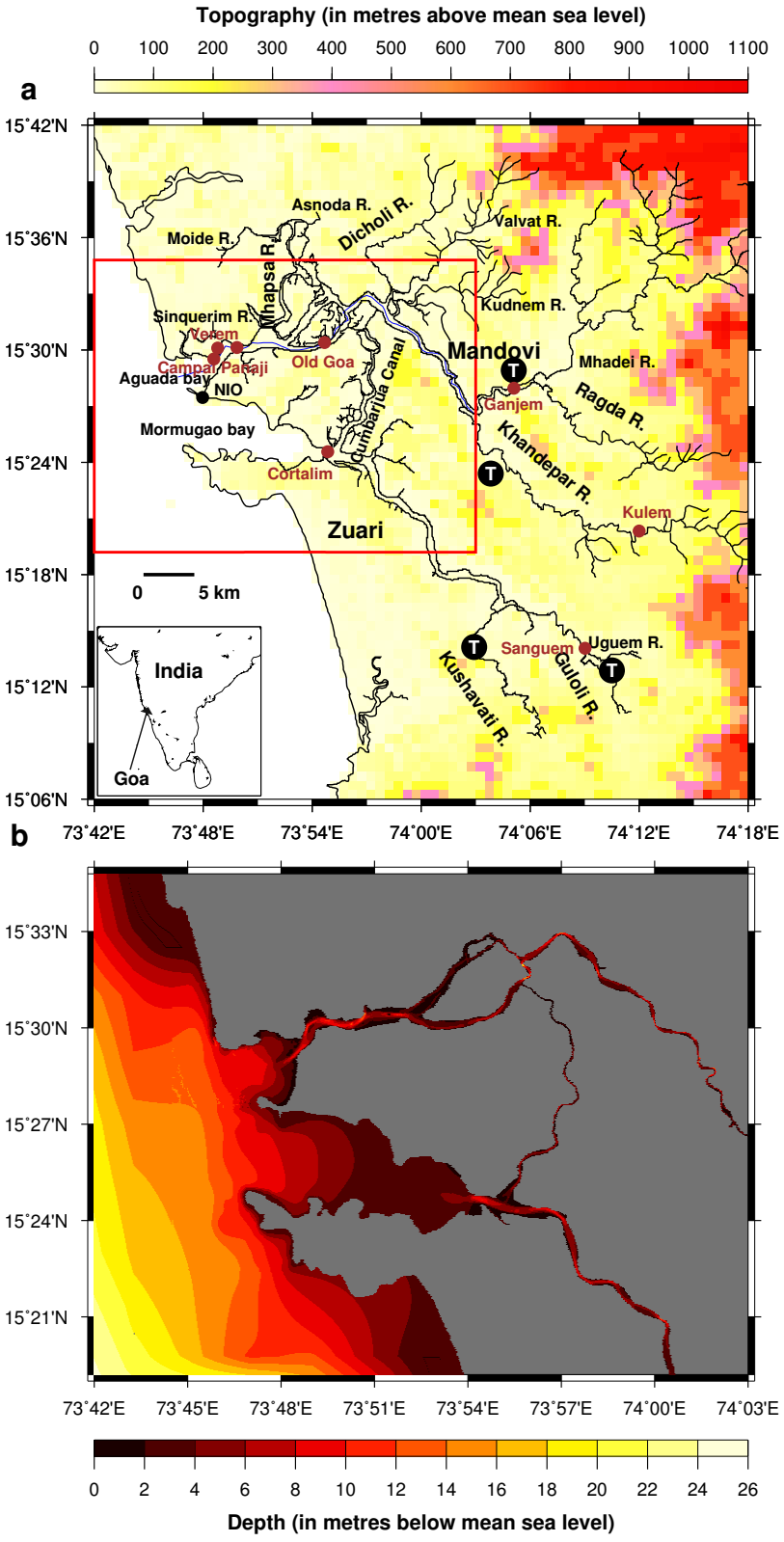

Figure 1:

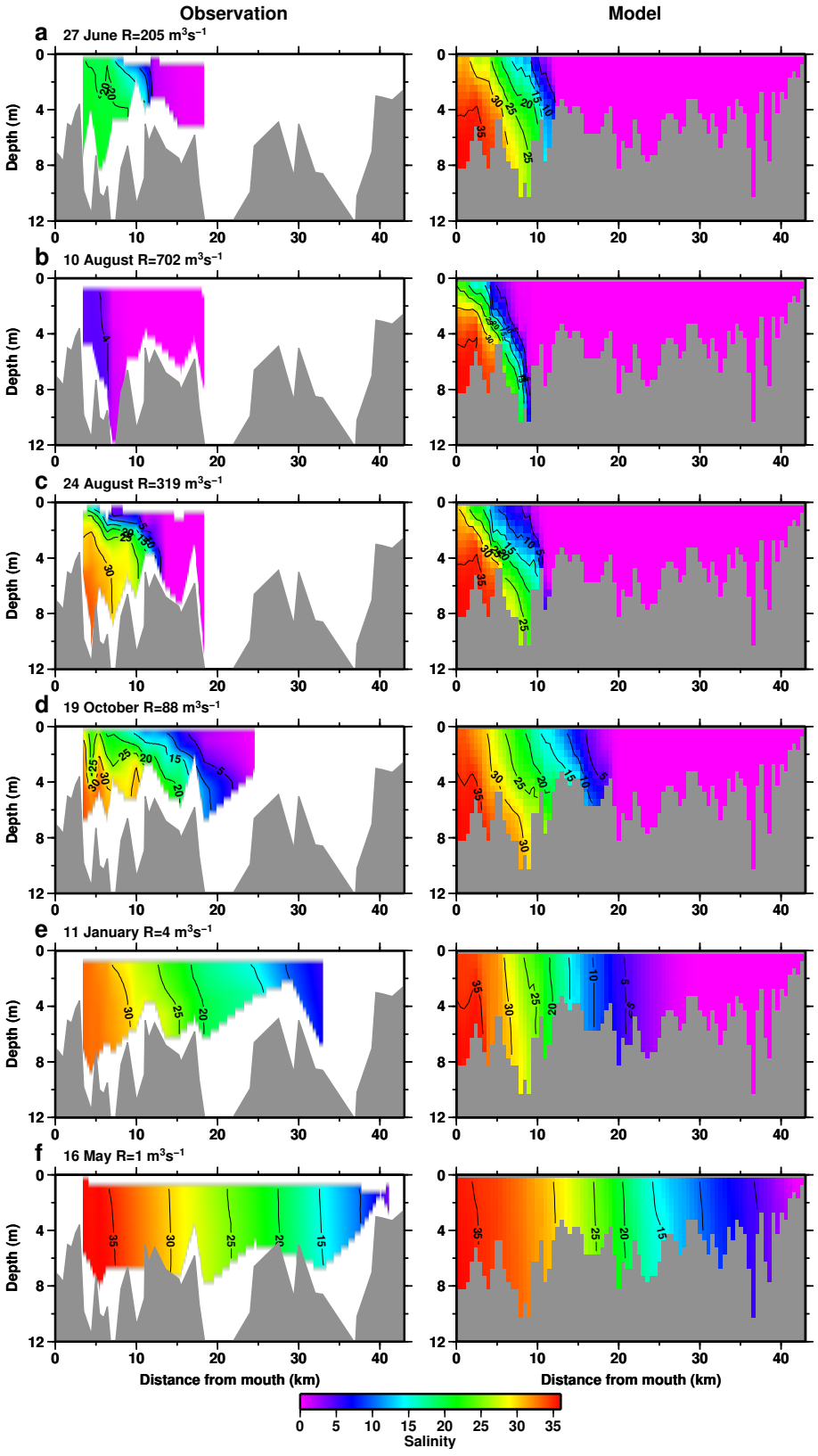
Observation
Model
a 27 June R=205 m3s−1
b 10 August R=702 m3s−1
c 24 August R=319 m3s−1
d 19 October R=88 m3s−1
e 11 January R=4 m3s−1
f 16 May R=1 m3s−1
Depth (m)
Distance from mouth (km)
Salinity

Figure 2:

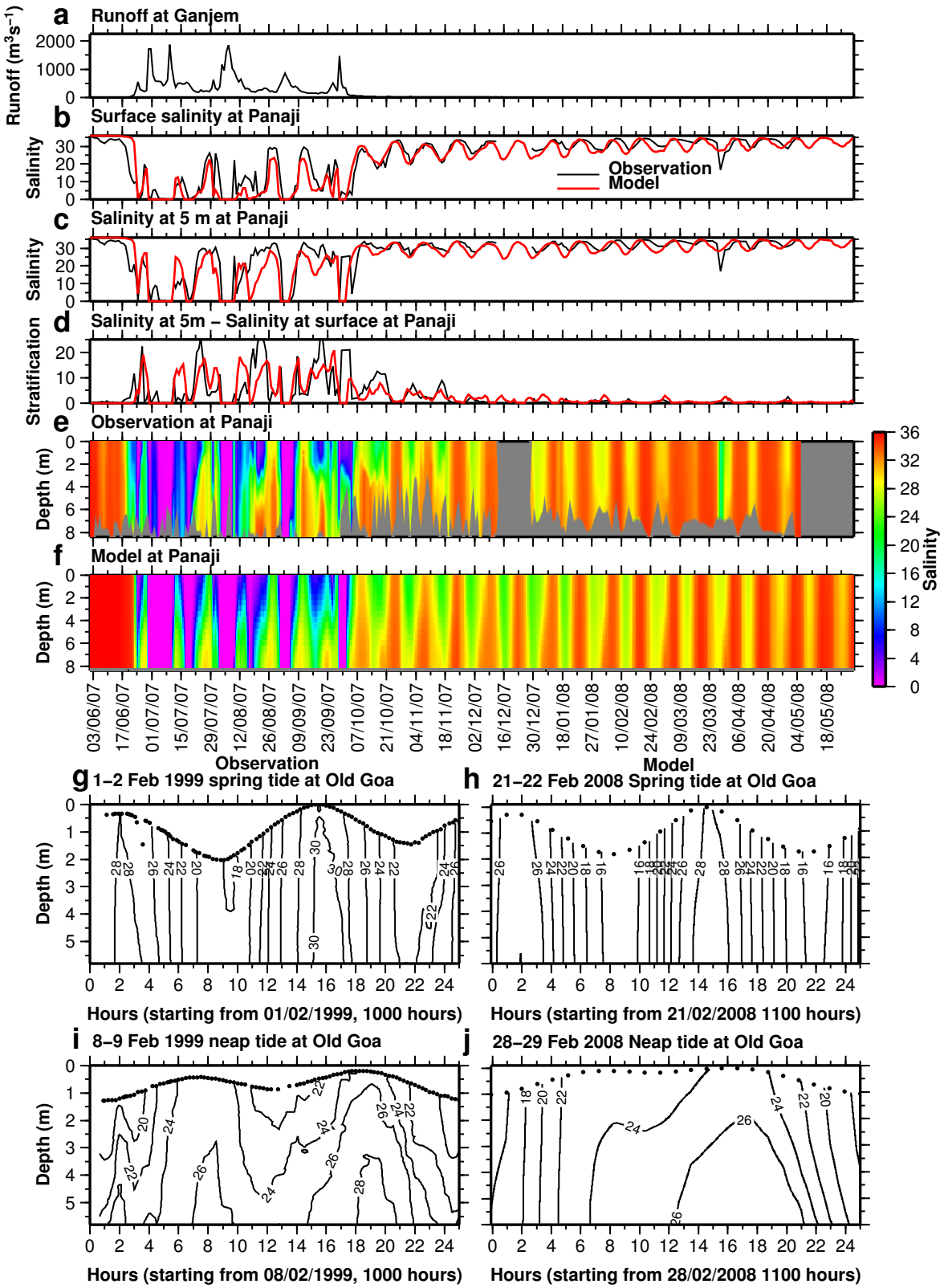
a
Runoff at Ganjem
Runoff (m3s−1)
2000
1000
0
b
Surface salinity at Panaji
Salinity
30
20
10
0
Observation
Model
c
Salinity at 5 m at Panaji
Salinity
30
20
10
0
d
Salinity at 5m – Salinity at surface at Panaji
Stratification
20
10
0
e
Observation at Panaji
Depth (m)
0
2
4
6
8
f
Model at Panaji
Depth (m)
0
2
4
6
8
36
32
28
24
20
16
12
8
4
0
Salinity
03/06/07
17/06/07
01/07/07
15/07/07
29/07/07
12/08/07
26/08/07
09/09/07
23/09/07
07/10/07
21/10/07
04/11/07
18/11/07
02/12/07
16/12/07
30/12/07
18/01/08
27/01/08
10/02/08
24/02/08
09/03/08
23/03/08
06/04/08
20/04/08
04/05/08
18/05/08
Observation
g
1–2 Feb 1999 spring tide at Old Goa
Depth (m)
Hours (starting from 01/02/1999, 1000 hours)
Model
h
21–22 Feb 2008 Spring tide at Old Goa
Hours (starting from 21/02/2008 1100 hours)
i
8–9 Feb 1999 neap tide at Old Goa
Depth (m)
Hours (starting from 08/02/1999, 1000 hours)
j
28–29 Feb 2008 Neap tide at Old Goa
Hours (starting from 28/02/2008 1100 hours)

Figure 3:

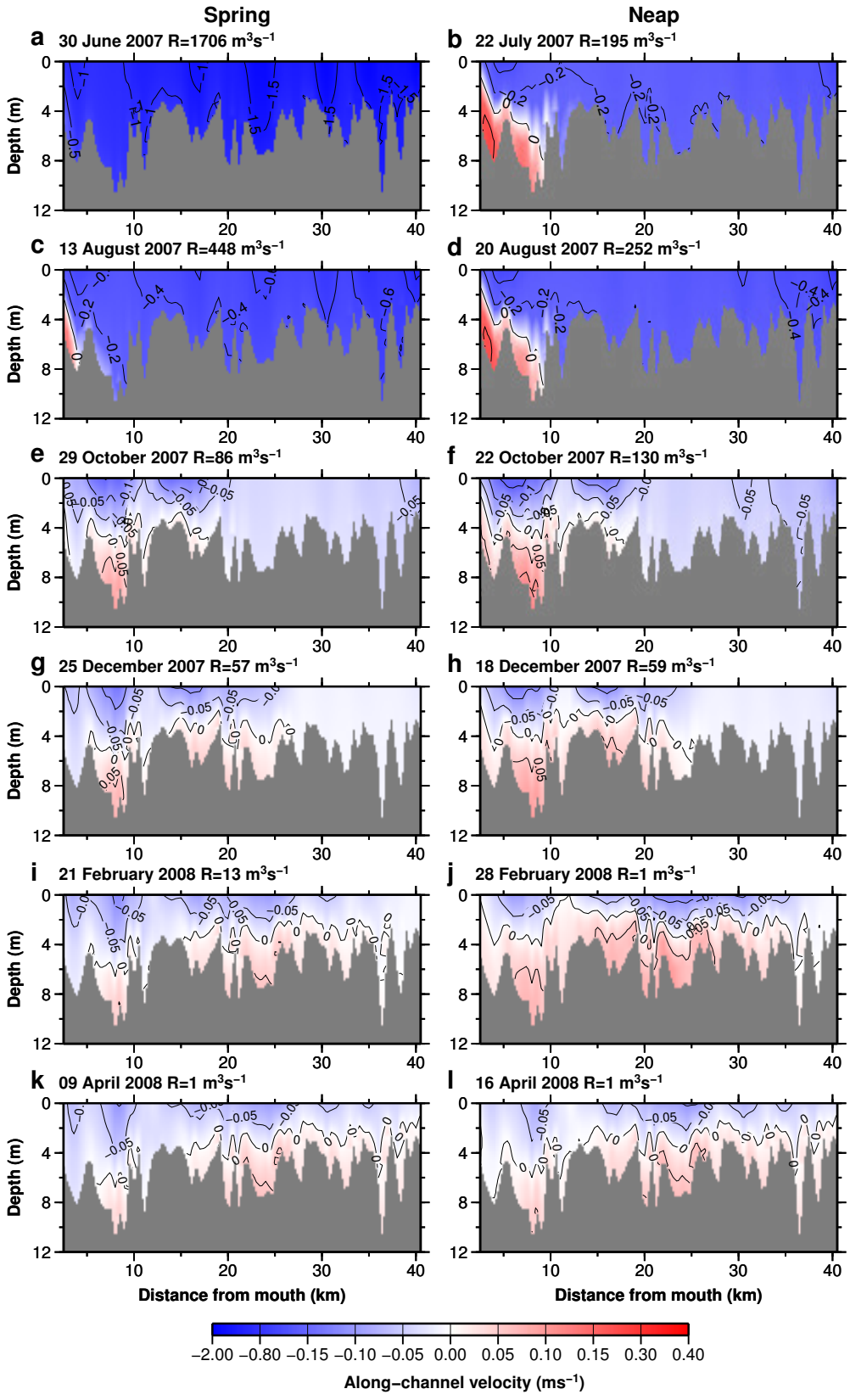
Spring
Neap
a 30 June 2007 R=1706 m³s⁻¹
b 22 July 2007 R=195 m³s⁻¹
c 13 August 2007 R=448 m³s⁻¹
d 20 August 2007 R=252 m³s⁻¹
e 29 October 2007 R=86 m³s⁻¹
f 22 October 2007 R=130 m³s⁻¹
g 25 December 2007 R=57 m³s⁻¹
h 18 December 2007 R=59 m³s⁻¹
i 21 February 2008 R=13 m³s⁻¹
j 28 February 2008 R=1 m³s⁻¹
k 09 April 2008 R=1 m³s⁻¹
l 16 April 2008 R=1 m³s⁻¹
Depth (m)
Distance from mouth (km)
−2.00 −0.80 −0.15 −0.10 −0.05 0.00 0.05 0.10 0.15 0.30 0.40
Along−channel velocity (ms⁻¹)

Figure 4:

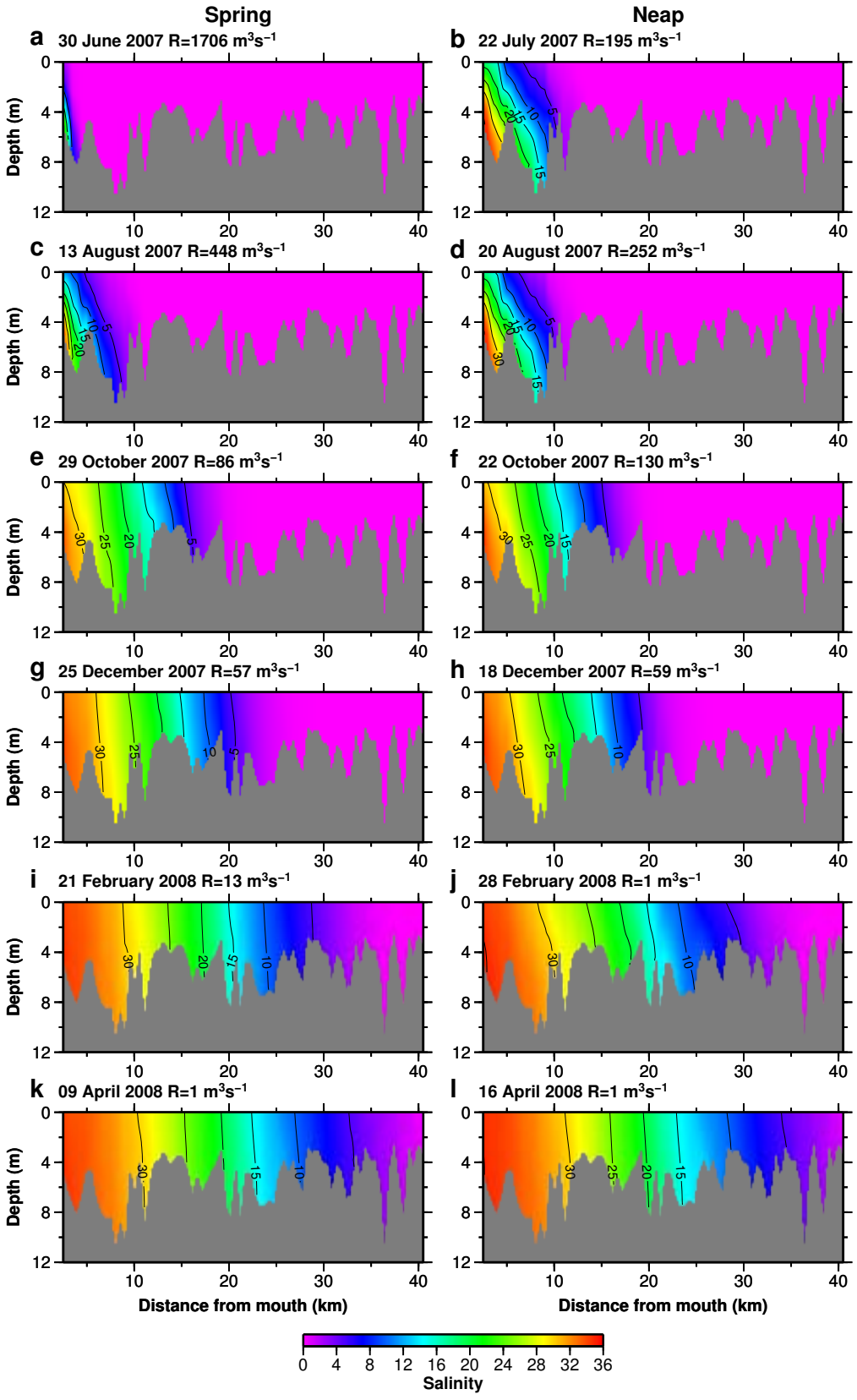
Spring
Neap
a 30 June 2007 R=1706 m³s⁻¹
b 22 July 2007 R=195 m³s⁻¹
c 13 August 2007 R=448 m³s⁻¹
d 20 August 2007 R=252 m³s⁻¹
e 29 October 2007 R=86 m³s⁻¹
f 22 October 2007 R=130 m³s⁻¹
g 25 December 2007 R=57 m³s⁻¹
h 18 December 2007 R=59 m³s⁻¹
i 21 February 2008 R=13 m³s⁻¹
j 28 February 2008 R=1 m³s⁻¹
k 09 April 2008 R=1 m³s⁻¹
l 16 April 2008 R=1 m³s⁻¹
Depth (m)
Distance from mouth (km)
Salinity

Figure 5:

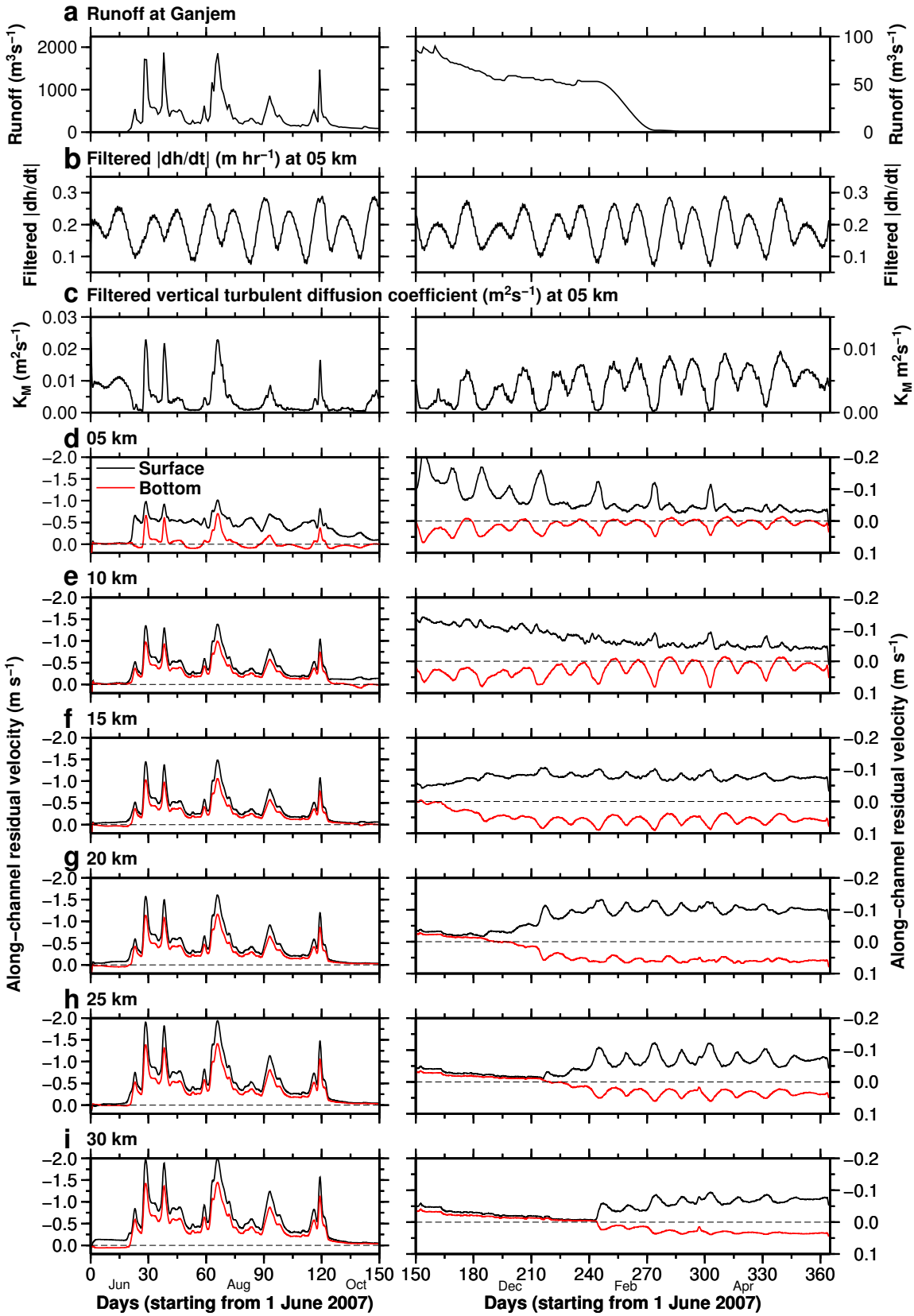
a Runoff at Ganjem
Runoff (m3s−1)
b Filtered |dh/dt| (m hr−1) at 05 km
Filtered |dh/dt|
c Filtered vertical turbulent diffusion coefficient (m2s−1) at 05 km
KM (m2s−1)
d 05 km
Surface
Bottom
e 10 km
f 15 km
g 20 km
h 25 km
i 30 km
Along−channel residual velocity (m s−1)
Jun
Aug
Oct
Dec
Feb
Apr
Days (starting from 1 June 2007)
Days (starting from 1 June 2007)

Figure 6:

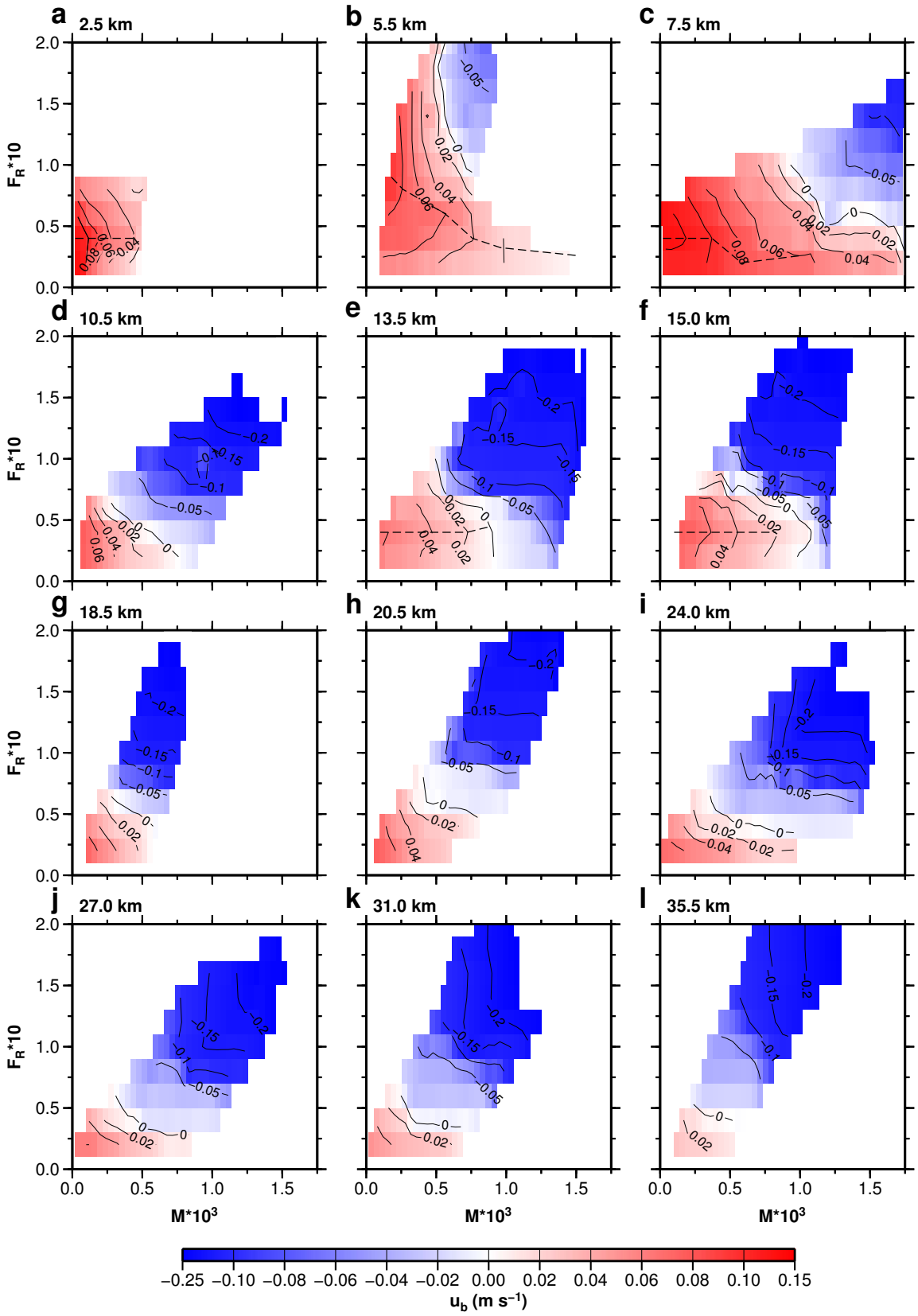
a 2.5 km
b 5.5 km
c 7.5 km
d 10.5 km
e 13.5 km
f 15.0 km
g 18.5 km
h 20.5 km
i 24.0 km
j 27.0 km
k 31.0 km
l 35.5 km
F_R*10
M*10^3
u_b (m s^-1)
−0.25 −0.10 −0.08 −0.06 −0.04 −0.02 0.00 0.02 0.04 0.06 0.08 0.10 0.15

Figure 7:

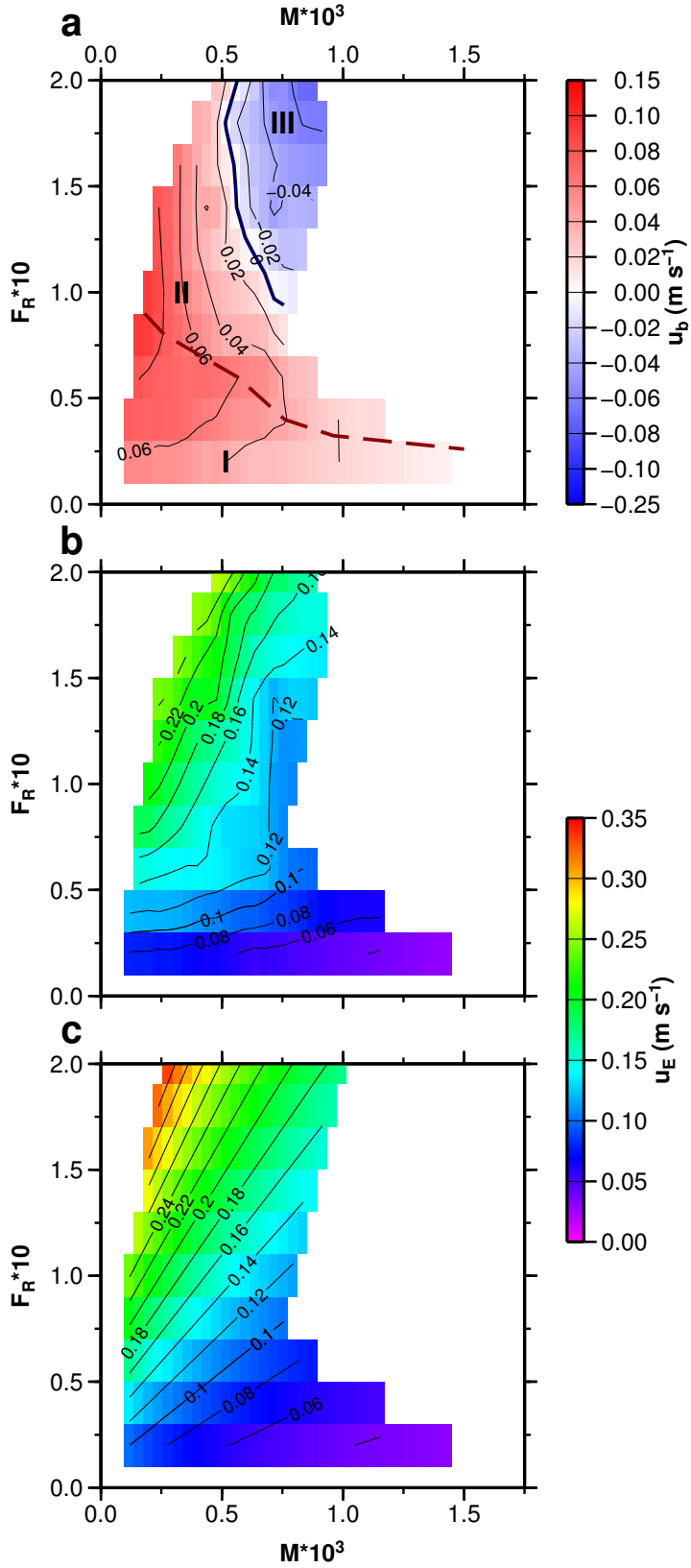

Figure 8:

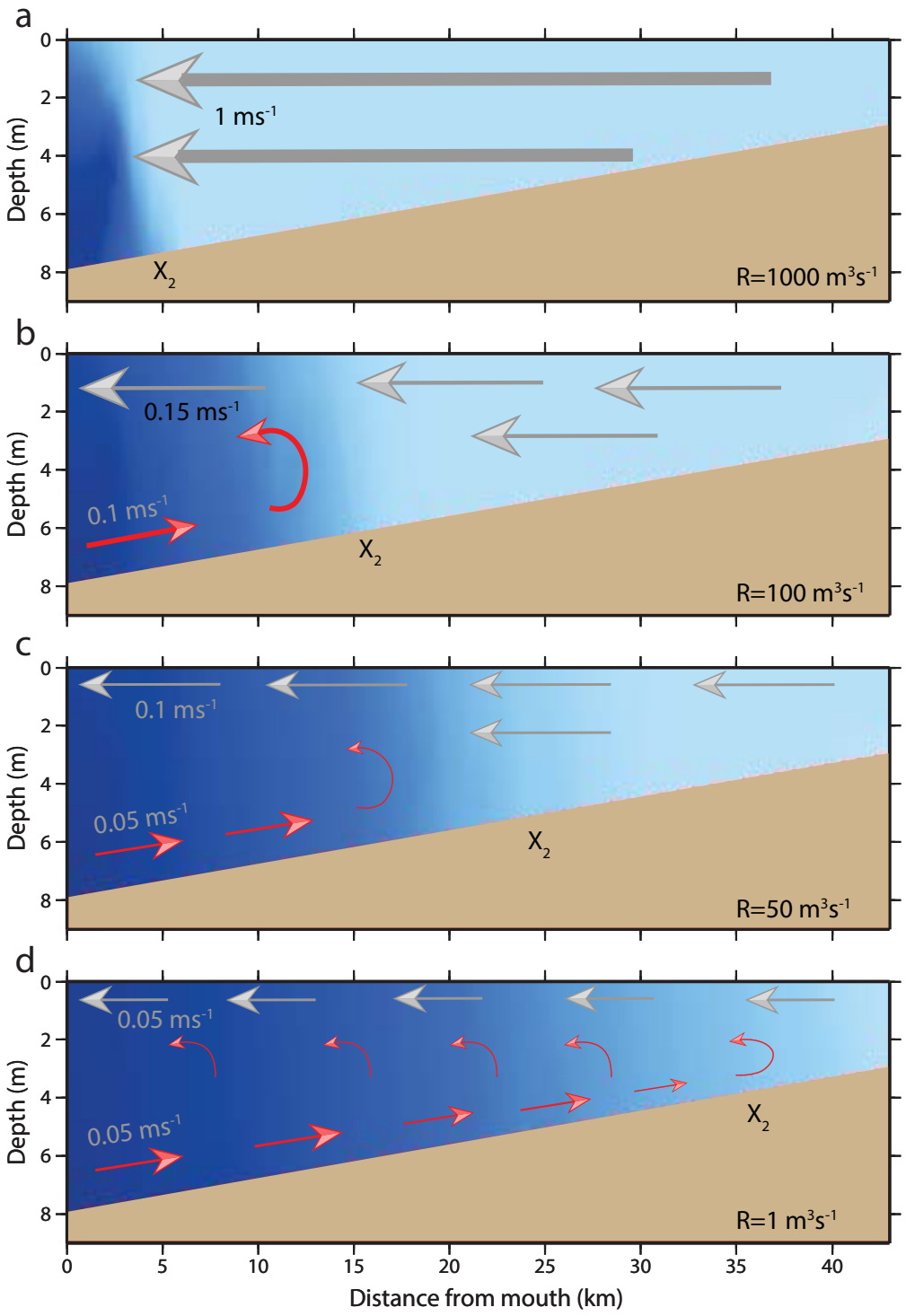
a
b
c
d
Depth (m)
0
2
4
6
8
1 ms-1
0.15 ms-1
0.1 ms-1
0.05 ms-1
0.05 ms-1
0.1 ms-1
X2
R=1000 m3s-1
R=100 m3s-1
R=50 m3s-1
R=1 m3s-1
0
5
10
15
20
25
30
35
40
Distance from mouth (km)

Figure 9: